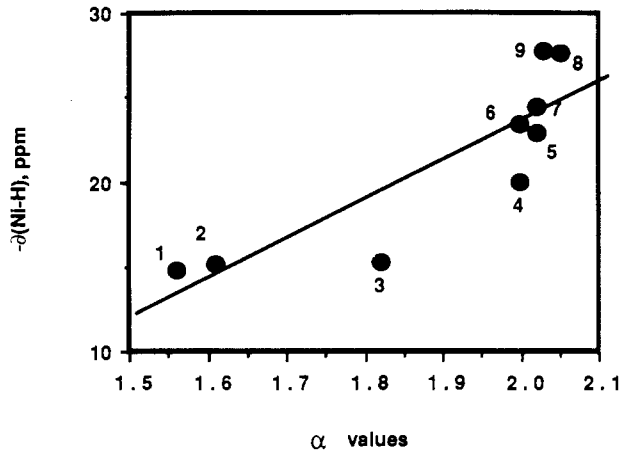

Figure 4. Plot of $-\delta$(Ni–H) vs α values[14] for *trans*-$HNi(X)(PCy_3)_2$. X is Ph (1), Me (2), CN (3), I (4), Br (5), SCN (6), Cl (7), HCO_2 (8), and AcO (9).

Spectroscopic scales have been developed for other complex geometries. Marzilli tabulated (as τ values) the chemical shifts of the α-proton of the *tert*-butylpyridine ligand trans to the substituents, X, in the Co(III) complexes $LCo(DH)_2X$ (L = 4-*tert*-butylpyridine and DH = $HONC(CH_3)C(CH_3)NO^-$) and reported these spectroscopic substituent constants as a proton NMR spectrochemical series.[12] Smaller α values were noted for soft carbon-donor ligands, and values increased with the hardness of the substituent: Ph (α = 1.56) < CH_3 (1.61) < SCN (1.96) < I (2.00) < Cl, Br (2.02) < OAc (2.03) < F (2.24). The transferability was shown in that the α-values correlate with the platinum–hydrogen stretching frequency in *trans*-$HPt(X)L_2$ and the Pt–C–H coupling constant in *trans*-$Pt(CH_3)(X)L_2$.[13] A plot of Marzilli's α values vs nickel–hydride chemical shifts of our series (Figure 4) further supports the transferability of such substituent constants. It is interesting to note that the same trends exist in coordination complexes of Co(III) and the "softer" coordination sphere of the nickel(II) and platinum(II) phosphines studied in other laboratories.

The wide range of nickel–hydrogen bond strengths is evidenced by reactivity with MeI and CO_2. Both react with carbon-bound derivatives preferentially at the hydride ligand. The sulfur- and oxygen-bound derivatives show no reactivity at the hydride. Iodomethane reacts preferentially at the ligands with easily accessible lone pairs, alkylating the ligand and leaving the hydride intact. Carbon dioxide shows no reactivity with the sulfur and oxygen derivatives at either the NiH or NiX sites.[14]

Acknowledgment. The financial support of the Robert A. Welch Foundation is greatly appreciated. In addition, we acknowledge Lai Y. Goh's assistance in our initial syntheses and the helpful comments of D. J. Darensbourg.

(12) Marzilli, L. G.; Politzer, P.; Trogler, W. C.; Stewart, R. C. *Inorg. Chem.* **1975**, *14*, 2389.

(13) Appleton, T. G.; Clark, H. C.; Manzer, L. E. *Coord. Chem. Rev.* **1973**, *10*, 335.

(14) (a) Newman, L. J.; Bergman, R. G. *J. Am. Chem. Soc.* **1985**, *107*, 5314. (b) No reaction of **5** with CO_2 was observed even under 1000 psi of CO_2: Darensbourg, D. J.; Wiegreffe, P. W. Unpublished results.

Contribution from the Department of Chemical Engineering, The Pennsylvania State University, University Park, Pennsylvania 16802

DRIFTS Investigation of the Decomposition of Ruthenium Clusters on Carbon and the Subsequent Ruthenium/Carbon Catalysts

Jeremy J. Venter and M. Albert Vannice*

Received August 5, 1988

The thermal decomposition of $Ru_3(CO)_{12}$ has been studied for the first time by dispersing this cluster on an oxygen-free carbon support and using diffuse reflectance infrared Fourier transform spectroscopy (DRIFTS). The $Ru_3(CO)_{12}$ clusters on carbon decomposed straightforwardly in He but transformed to $H_4Ru_4(CO)_{12}$ during decarbonylation in H_2. First-order rate constants of decomposition in He and H_2 were determined for each cluster, compared to literature values for nucleophilic substitution in solution, and found to be similar. This implies that the rate-determining step in these decomposition reactions appears to be the same as that in substitution reactions—removal of the first CO ligand. The activation energy of decarbonylation of $Ru_3(CO)_{12}$ was near 20.5 kcal/mol in He, while $Ru_3(CO)_{12}$ and $H_4Ru_4(CO)_{12}$ had values of 18–22 kcal/mol in H_2. These activation energies are lower than those observed for substitution reactions in solution, but this can be explained by considering Ru–Ru bond formation during the decomposition process to give highly dispersed metallic Ru crystallites. Chemisorption measurements confirmed the presence of very small Ru particles on carbon following decomposition at 673 K under either He or H_2, and the DRIFTS spectra of CO chemisorbed on these Ru crystallites indicated the presence of zerovalent Ru. The resulting Ru/C catalysts exhibited low CO hydrogenation turnover frequencies consistent with values in the literature for very small Ru crystallites on inert supports. The isothermal, integral heat of adsorption of CO was measured calorimetrically at 300 K and found to be 24.2 ± 1.6 kcal/mol. This study is part of the first successful application of an IR spectroscopic technique to characterize carbon-supported metals.

Introduction

A significant interest in carbon as a support for metal catalysts presently exists,[1-16] primarily because amorphous carbons can be prepared with high surface areas of over 1000 m^2/g and can stabilize highly dispersed Ru, Co, Fe, and Mn particles.[1-7] These carbons can be highly dehydroxylated and decarboxylated, and they possess the capability to stabilize highly dispersed crystallites in metallic form in the absence of surface functional groups which are typically present on ordinary oxide supports.[17] These highly dispersed metals have been shown to be very active and, in some cases, quite unique CO hydrogenation catalysts.[1-7] Electronic interactions in these metal–carbon systems have been pro-

* To whom correspondence should be sent.

(1) Jung, H. J.; Vannice, M. A.; Mulay, L. N.; Stanfield, R. M.; Delgass, W. N. *J. Catal.* **1982**, *76*, 208.
(2) Niemantsverdriet, J. W.; van der Kraan, A. M.; Delgass, W. N.; Vannice, M. A. *J. Phys. Chem.* **1985**, *89*, 67.
(3) Kaminsky, M.; Yoon, K. J.; Geoffroy, G. L.; Vannice, M. A. *J. Catal.* **1985**, *91*, 338.
(4) Chen, A.; Kaminsky, M.; Geoffroy, G. L.; Vannice, M. A. *J. Phys. Chem.* **1986**, *90*, 4810.
(5) Venter, J. J.; Kaminsky, M.; Geoffroy, G. L.; Vannice, M. A. *J. Catal.* **1987**, *103*, 450.
(6) Venter, J. J.; Kaminsky, M.; Geoffroy, G. L.; Vannice, M. A. *J. Catal.* **1987**, *105*, 155.

0020-1669/89/1328-1634$01.50/0

posed,[13,18,19] but the exact nature of the surface chemistry remains unclear.[7]

The interaction of metal carbonyl clusters (MCC's) with different supports can be a valuable technique to elucidate the character of the support surface. MCC-derived Rh,[20,21] Os,[22-26] and Ir[27-29] catalysts have given information about the influence of pretreatment conditions of the support on the stability of these clusters. Until recently these studies had been done using metal oxide supports and transmission infrared (IR) spectroscopy as the major technique; however, with the development of diffuse reflectance infrared Fourier transform spectroscopy (DRIFTS) it has now become possible to investigate carbon-supported MCC's by using IR spectroscopy.[30,31] Although $Os_3(CO)_{12}$ and Os MCC's in general are very well characterized due to their exceptional stability,[22-26] a significant amount of work has also been done on $Ru_3(CO)_{12}$ and other Ru MCC's. These clusters have been stabilized on functionalized polymers,[32] functionalized oxides,[33-36] and oxide supports,[37-42] and they have been well characterized in solution, thereby providing a wealth of background information. Furthermore, Ru is known to be one of the most active catalysts for CO hydrogenation,[43-46] and the kinetics of this reaction have been thoroughly studied, thereby providing a sound basis for comparison.

In order to extend the existing knowledge of both carbon-supported Ru and the chemistry associated with the decarbonylation of MCC's, a DRIFTS investigation was undertaken to closely monitor the decomposition of $Ru_3(CO)_{12}$ on an amorphous carbon black free of oxygen-containing surface groups. The quantitative rates of decarbonylation of $Ru_3(CO)_{12}$ in both He and H_2 and the adsorption of CO on the residual metallic particles, as well as the differences between these results and those reported for oxide-supported Ru systems, were examined. This cluster-derived, carbon-supported Ru catalyst was also characterized by using CO and H_2 chemisorption, and the activity for CO hydrogenation was determined and compared to reported activities. Finally, the integral heat of adsorption (Q_{ad}) of CO on small Ru crystallites at 300 K was determined for the first time and compared to values reported for single-crystal surfaces.

Table I. Chemisorption Measurements on 8.3 wt % Ru/C Catalysts Derived from $Ru_3(CO)_{12}$

	fresh cat[a]		used cat[a]	
	uptake, μmol/g of cat	H/Ru_t or CO/Ru_t	uptake, μmol/g of cat	H/Ru_t or CO/Ru_t
	LTR			
H_2(0–200 °C)	44	0.11		
CO(195 K)	332	0.41		
CO(300 K)	462	0.57		
CO(300)/CO(195)	1.4			
	HTR			
H_2(0–400 °C)	65	0.16	74	0.18
CO(195 K)	289	0.35	260	0.32
CO(300 K)	302	0.37	242	0.30
CO(300)/CO(195)	1.0		0.9	

[a] Ru_t is the total number of Ru atoms.

Experimental Section

Catalyst Preparation. The amorphous carbon black used as a support in this study was CSX-203 from Cabot Corp. (now available as Black Pearls 2000). Sulfur and oxygen were removed from the surface by treatment in H_2 at 1223 K for 12 h,[1,47] and this high-temperature-treated carbon was then stored in a glovebox to avoid air exposure. Before the support was impregnated with the carbonyl cluster, the carbon was heated to 673 K under dynamic vacuum (10^{-4} kPa) for 8 h. The $Ru_3(CO)_{12}$ was purchased from Strem Chemical Co. and used without further purification. $Ru_3(CO)_{12}$ was dispersed on the carbon by an incipient wetness impregnation technique by using dry, degassed THF as solvent (20 cm^3/g C), introducing the solution under nitrogen by using standard Schlenk techniques,[48] and removing the solvent by evacuating to 10^{-4} kPa for 8 h at 300 K. The catalyst was then stored in a glovebox under N_2.

DRIFTS Investigation. The infrared spectra were collected on a N_2-purged, Mattson Instruments Sirius 100 FTIR using an extensively modified version of a Harrick Scientific HVC-DRP DRIFTS cell, which was coupled to a praying mantis mirror assembly (DRA-2CS, Harrick Scientific) as discussed elsewhere.[49] The DRIFTS samples were obtained by mixing the carbon-supported Ru catalyst with precalcined, H_2-pretreated CaF_2 inside the glovebox and using a CaF_2:C dilution ratio of 200:1. Portions of this sample were used to load the DRIFTS cell inside the glovebox prior to connecting the cell to the FTIR spectrometer without air exposure.

The rates of decarbonylation were measured in H_2 and also in He, after which the sample was heated to 673 K in the same gas for 10–16

(7) Chen, A. A.; Vannice, M. A.; Phillips, J. *J. Phys. Chem.* **1987**, *91*, 6257.
(8) Phillips, J.; Clausen, B.; Dumesic, J. A. *J. Phys. Chem.* **1980**, *84*, 1814.
(9) Phillips, J.; Dumesic, J. A. *Appl. Surf. Sci.* **1981**, *7*, 215.
(10) Lin, S. C.; Phillips, J. *J. Appl. Phys.* **1985**, *58*, 1943.
(11) Gatte, R. R.; Phillips, J. P. *J. Catal.* **1987**, *104*, 365.
(12) Bartholomew, C. H.; Boudart, M. *J. Catal.* **1973**, *29*, 278.
(13) Jones, V. K.; Neubauer, L. R.; Bartholomew, C. H. *J. Phys. Chem.* **1986**, *90*, 4832.
(14) Tau, L. M.; Bennett, C. O. *J. Phys. Chem.* **1986**, *90*, 4825.
(15) Reinoso, F. R.; Ramos, I. R.; Castilla, C. M.; Ruiz, A. G.; Gonzalez, J. D. L. *J. Catal.* **1986**, *99*, 171.
(16) Reinoso, F. R.; Ramos, I. R.; Ruiz, A. G.; Gonzalez, J. D. L. *Appl. Catal.* **1986**, *21*, 251.
(17) Phillips, J.; Dumesic, J. A. *Appl. Catal.* **1984**, *9*, 1.
(18) Hegenberger, E.; Wu, N. L.; Phillips, J. *J. Phys. Chem.* **1987**, *91*, 5067.
(19) Rodriguez-Ramos, I.; Rodriguez-Reinoso, F.; Guerrero-Ruiz, A.; Lopez-Gonzalez, J. *J. Chem. Technol. Biotechnol.* **1986**, *36*, 67.
(20) Bilhou, J. L.; Bilhou-Bougnol, V.; Graydon, W. F.; Basset, J. M.; Smith, A. K.; Zanderighi, G. M.; Ugo, R. *J. Organomet. Chem.* **1987**, *153*, 73.
(21) Theolier, A.; Smith, A. K.; Leconte, M.; Basset, J. M.; Zanderighi, G. M.; Psaro, R.; Ugo, R. *J. Organomet. Chem.* **1980**, *191*, 415.
(22) Psaro, R.; Dossi, C.; Ugo, R. *J. Mol. Catal.* **1983**, *21*, 331.
(23) Psaro, R.; Ugo, R.; Zanderighi, G. M.; Besson, B.; Smith, A. K.; Basset, J. M. *J. Mol. Catal.* **1981**, *21*, 215.
(24) Lamb, H. H.; Gates, B. C. *J. Am. Chem. Soc.* **1986**, *108*, 81.
(25) Basset, J. M.; Choplin, A. *J. Mol. Catal.* **1983**, *21*, 95.
(26) Deeba, M.; Gates, B. C. *J. Catal.* **1981**, *67*, 303.
(27) Rafalko, J. J.; Lieto, J.; Gates, B. C.; Schrader, G. L. *J. Chem. Soc., Chem. Commun.* **1978**, 1063.
(28) Lieto, J.; Rafalko, J. J.; Gates, B. C. *J. Catal.* **1980**, *62*, 149.
(29) Wolf, M.; Lieto, B. A.; Matrana, B. A.; Arnold, D. B.; Gates, B. C.; Knozinger, H. *J. Catal.* **1984**, *89*, 100.
(30) Venter, J. J.; Vannice, M. A. *J. Am. Chem. Soc.* **1987**, *109*, 6204.
(31) Venter, J. J.; Vannice, M. A. *J. Am. Chem. Soc.*, in press.
(32) Otero-Schipper, Z.; Lieto, J.; Gates, B. C. *J. Catal.* **1980**, *63*, 175.
(33) Pierantozzi, R.; McQuade, K. J.; Gates, B. C.; Wolf, M.; Knozinger, H.; Ruhmann, W. *J. Am. Chem. Soc.* **1979**, *101*, 5436.
(34) Catrillo, T.; Knozinger, K.; Wolf, M. *Inorg. Chim. Acta* **1980**, *45*, L235.
(35) Evans, J.; Gracey, B. P. *J. Chem. Soc., Chem. Commun.* **1980**, 852.
(36) Gallezot, P.; Coudurier, G.; Primet, M.; Imelik, B. *ACS Symp. Ser.* **1977**, *No. 40*, 144.
(37) Dobos, S.; Boszormenyi, I.; Mink, J.; Guczi, L. *Inorg. Chim. Acta* **1986**, *120*, 135.
(38) Dobos, S.; Boszormenyi, I.; Mink, J.; Guczi, L. *Inorg. Chim. Acta* **1986**, *120*, 145.
(39) Kuznetsov, V.; Bell, A. T.; Yermakov, Y. I. *J. Catal.* **1980**, *65*, 374.
(40) Zecchina, A.; Guglielminotti, E.; Bossi, A.; Camia, M. *J. Catal.* **1982**, *74*, 225.
(41) Guglielminotti, E.; Zecchina, A.; Bossi, A.; Camia, M. *J. Catal.* **1982**, *74*, 240.
(42) Guglielminotti, E.; Zecchina, A.; Bossi, A.; Camia, M. *J. Catal.* **1982**, *74*, 252.
(43) Boudart, M.; McDonald, M. A. *J. Phys. Chem.* **1984**, *88*, 2185.
(44) Vannice, M. A. *Catal.: Sci. Technol.* **1982**, *3*, 140.
(45) Vannice, M. A. *Catal. Rev.—Sci. Eng.* **1976**, *14*, 153.
(46) Vannice, M. A.; Garten, R. L. *J. Catal.* **1980**, *63*, 255.
(47) Anderson, R. B.; Emmett, P. H. *J. Phys. Chem.* **1952**, *56*, 753.
(48) Shriver, D. F. *The Manipulation of Air Sensitive Compounds*; Wiley: New York, 1969.
(49) Venter, J. J.; Vannice, M. A. *Appl. Spectrosc.* **1988**, *42*, 1096.

Table II. Kinetic Behavior of Ru/C Derived from $Ru_3(CO)_{12}$

	activity,[a] μmol of CO/g of cat·s pretreatment		turnover freq,[a] 10^3 s^{-1} pretreatment		activation energy kcal/mol		partial pressure dependency[b]	
	LTR	HTR	LTR	HTR[c]	LTR	HTR	x	y
CO(tot.)	2.174	1.743	6.6	6.0	24.4	22.0		
$CO-CO_2$	0.060	0.046	0.2	0.2	23.9	22.7	0.0	0.3
CO–HC	2.114	1.697	6.4	5.9	24.4	22.0	0.9	0.0
$CO-CH_4$	2.114	1.697	6.4	5.9	24.4	22.0	0.9	0.0

[a] H_2:CO = 3:1; P = 0.1 M Pa; T = 548 K. [b] $r = kP_{H_2}{}^{x}P_{CO}{}^{y}$; T = 537 K. [c] Based on CO chemisorption at 195 K, assuming CO:Ru = 1:1.

h in order to allow the collection of spectra of adsorbed CO on the fully decarbonylated catalyst. The Ru/C catalyst was also investigated under reaction conditions following a high-temperature-reduction (HTR) step of 16 h at 673 K under 1 atm of flowing H_2. Spectra were collected at 473, 523, and 573 K in flowing CO (11 Torr) and H_2 (749 Torr). The fully decarbonylated catalyst in the absence of CO was used as the background reference material in all cases. The FTIR parameters were set to obtain a resolution of 4 cm^{-1}. The decarbonylation spectra were obtained by averaging 1000 scans, whereas the CO adsorption and reaction spectra were obtained by signal-averaging 10000 scans. The background spectra in all cases were obtained by averaging 10000 scans.

The data manipulation consisted of ratioing the sample and background spectra to obtain the transmittance spectra, calculating the absorbance spectra, base-line-correcting the absorbance files, transforming these files to obtain base-line-corrected transmittance files, and finally calculating the diffuse-reflectance files (in Kubelka–Munk units) from the base-line-corrected transmittance files. Both absorbance and Kubelka–Munk (K–M) spectra were plotted to check for consistency in base-line-correction. They were invariably nearly identical, so the spectra presented in this section will be only in K–M units, i.e., $KM = (1 - R_0)^2/(2R_0) = kc/s$, where R_0 is the base-line-corrected transmittance spectrum $[R_{sample}/R_{bkgd}]$, k is the molar extinction coefficient, c is the concentration, and s is a scattering coefficient.[50] In a previous study it was shown that peak intensities were directly proportional to cluster concentrations at these loadings and lower; i.e., both k and s values remained constant.[51]

Chemisorption, Kinetic, and Calorimetric Measurements. The apparatus used in this study has been described elsewhere.[49] CO and H_2 chemisorptions on the fresh catalyst were measured after a low-temperature-reduction (LTR) step (473 K for 2 h) in flowing H_2 as well as a HTR step (673 K for 16 h), whereas the used samples after the kinetic study were characterized following a HTR pretreatment.[4,5] CO chemisorption was determined by using the dual isotherm method,[52] while desorption after cooling in H_2 to 300 K and evacuating was used to determine H_2 uptakes.[53] The kinetic measurements were obtained at 1 atm under differential conditions by using a glass, plug-flow microreactor system.[1] The activities were obtained after either LTR or HTR by using a bracketing technique to avoid deactivation,[54] and partial pressure analyses were performed after HTR by using He as the diluent. The isothermal energy changes upon adsorption of CO were measured by using a modified Perkin-Elmer DSC-2C differential scanning calorimeter.[55-57] The only additional modification made was the installation of a small glovebox on the DSC, which allowed the transfer of catalyst into the DSC without air exposure. Calorimetric and adsorption measurements were done in parallel on samples derived from a single batch of catalyst by using identical treatments in each system, which provided reproducible heats of adsorption on two samples. Details of the experimental procedure are described elsewhere.[31]

Results

Chemisorption. The Ru weight loading was determined to be 8.3 wt % by slow ashing of the carbon support. This loading was in good agreement with the expected value calculated from the impregnation step.

Table III. Integral Heat of Adsorption of CO at 300 K on Reduced Carbon-Supported Ru Derived from $Ru_3(CO)_{12}$

run no.	energy change, mcal/g of cat	chemisorption, μmol of CO/g of cat	heat of ads, kcal/mol of CO	dispersion, CO/Ru_t
		Sample 1		
1	9134	368	24.8	0.45
2	8273	319	25.9	0.39
		Sample 2		
2	8256	375	22.0	0.46
av			24.2 ± 1.6[a]	0.43

[a] Standard deviation.

The chemisorption results are listed in Table I. The CO chemisorption values after LTR indicate that the Ru was well dispersed, but the CO uptake at 195 K after the first LTR was lower than that at 300 K following a second LTR. The H_2 uptake was significantly lower than either CO uptake after LTR. After HTR, the fresh catalyst again showed larger CO uptakes than H_2 but the irreversible CO uptakes at 195 and 300 K were now essentially the same, consistent with previous studies.[58-62] Assuming dissociative H_2 adsorption,[63] the H coverage after HTR was approximately half that of CO. The similarity of CO uptakes after HTR indicates that minimal sintering of the Ru occurred, and this small variation in chemisorption between fresh and used catalysts was very similar to that observed for carbon-supported Os.[31] The reduced Ru clusters were therefore quite stable under reaction conditions.

Kinetic Measurements. The kinetic data, summarized in Table II, show that CH_4 was the only hydrocarbon product detected. Small quantities of CO_2 were also produced after either LTR or HTR. An active catalyst was obtained after only a LTR, and a turnover frequency (TOF) of 0.0064 s^{-1} was obtained at 548 K for methanation based on CO adsorption at 195 K, and a subsequent HTR step decreased the TOF slightly to 0.0059 s^{-1}. The activation energies for the formation of CH_4 after LTR and HTR were 24.4 and 22.0 kcal/mol, respectively, and for the formation of CO_2 they were 23.9 and 22.7 kcal/mol, respectively. The partial pressure analysis revealed a near first-order dependence on H_2 and a zero-order dependence on CO. The activation energy for CH_4 formation is in excellent agreement with previous values reported for Ru, but partial pressure dependencies are typically higher than first order in H_2 and around negative first order in CO.[45,58] However, such shifts in pressure dependency along with the much lower TOF's and high selectivity to CH_4 have previously been found for C-supported Ru.[3,46]

Calorimetric Measurements. The calorimetrically determined CO heat of adsorption together with the energy changes and CO chemisorption values are shown in Table III. The chemisorption values on two different samples after similar treatments were in excellent agreement. It decreased with a second HTR treatment

(50) Krishnan, K.; Ferraro, J. R. *Fourier Transform Infrared Spectroscopy: Techniques Using Fourier Transform Interferometry*; Academic Press: New York, 1986; Vol. 3, pp 149.
(51) Venter, J. J.; Vannice, M. A. *Carbon* **1988**, *26*, 889.
(52) Emmett, P. H.; Brunauer, S. *J. Am. Chem. Soc.* **1937**, *59*, 310.
(53) Amelse, J. A.; Schwartz, L. H.; Butt, J. B. *J. Catal.* **1981**, *72*, 95.
(54) Vannice, M. A. *J. Catal.* **1975**, *37*, 449.
(55) Sen, B.; Chou, P.; Vannice, M. A. *J. Catal.* **1986**, *101*, 517.
(56) Vannice, M. A.; Sen, B.; Chou, P. *Rev. Sci. Instrum.* **1987**, *58*, 647.
(57) Chou, P.; Vannice, M. A. *J. Catal.* **1987**, *104*, 17.
(58) Bell, A. T. *Catal. Rev.—Sci. Eng.* **1981**, *23*, 203.
(59) Madey, T. E.; Menzel, D. *Jpn. J. Appl. Phys. Suppl. v2 pt2* **1974**, 229.
(60) Fuggle, J. C.; Madey, T. E.; Steinkilberg, M.; Menzel, D. *Surf. Sci.* **1975**, *52*, 521.
(61) Fuggle, J. C.; Umbach, E.; Feulner, P.; Menzel, D. *Surf. Sci.* **1977**, *64*, 69.
(62) Thomas, G. E.; Weinberg, W. H. *J. Chem. Phys.* **1979**, *70*, 954.
(63) Bonzel, H. P.; Krebs, H. J. *Surf. Sci.* **1982**, *117*, 639.

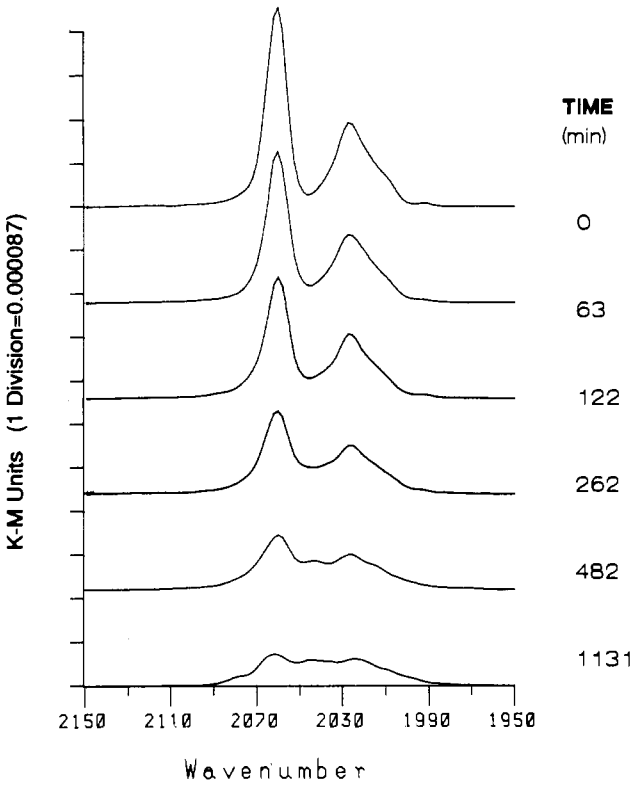

Figure 1. Spectra of carbon-supported $Ru_3(CO)_{12}$ after various times in He at 313 K. The principal IR bands are at 2060, 2027, and 2010 cm^{-1}.

from 368 to 319 μmol of CO/g of catalyst, but the heat released during adsorption decreased correspondingly to give reproducible Q_{ad} values, resulting in an average Q_{ad} of 24.2 kcal/mol of CO.

DRIFTS Measurements. Prior to the decarbonylation experiments, the spectrum of the carbon-supported $Ru_3(CO)_{12}$ was obtained in flowing He in order to ensure the presence of the intact cluster. The supported cluster remained intact for the duration of this study, and the observed bands of 2060, 2027, and 2010 cm^{-1} are in excellent agreement with values reported for the cluster in solution,[64-84] as shown in Table IV. After collection of this

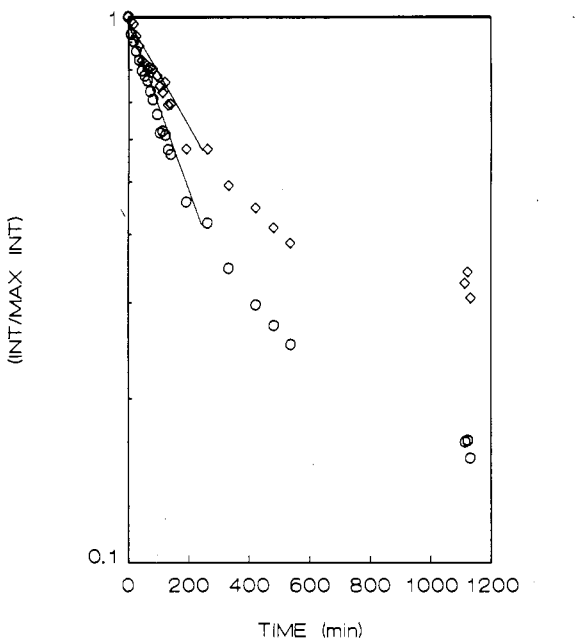

Figure 2. Rate of decarbonylation of carbon-supported $Ru_3(CO)_{12}$ in He at 313 K: ○, band at 2060 cm^{-1}; ◇, band at 2027 cm^{-1}.

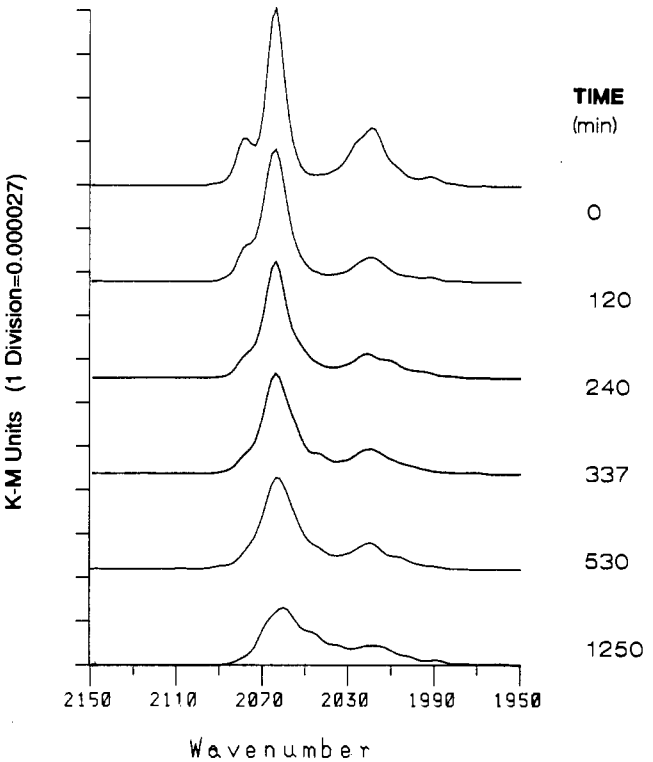

Figure 3. Spectra of carbon-supported $Ru_3(CO)_{12}$ after various times in H_2 at 338 K. The principal IR bands are at 2077, 2064, and 2021 cm^{-1}.

initial spectrum, the catalyst was heated rapidly in either He or H_2 to a constant temperature and the decarbonylation was followed as a function of time. Figure 1 shows the decarbonylation of carbon-supported $Ru_3(CO)_{12}$ in He at 313 K as a typical example. The initial spectrum in He at 313 K showed only three bands, in agreement with reported values for $Ru_3(CO)_{12}$ in solution. The cluster can be seen to decompose straightforwardly without significant transformation to another stable cluster. After the cluster was allowed to decompose for long periods of time at temperatures

(64) Dalla Betta, R. A. *J. Phys. Chem.* **1975**, *79*, 2519.
(65) Nicholls, J. N.; Farrar, D. H.; Jackson, P. F.; Johnson, B. F. G.; Lewis, J. *J. Chem. Soc., Dalton Trans.* **1982**, 1395.
(66) Calderazzo, F.; L'Eplattenier, F. *Inorg. Chem.* **1967**, *6*, 1220.
(67) Davydov, A. A.; Bell, A. T. *J. Catal.* **1977**, *49*, 332.
(68) Goodwin, J. G.; Naccache, C. *J. Mol. Catal.* **1982**, *14*, 259.
(69) Johnson, B. F. G.; Johnson, R. D.; Lewis, J. *J. Chem. Soc. A* **1969**, 792.
(70) Boszormenyi, I.; Dobos, S.; Guczi, L.; Marko, L.; Reiff, W. M. *Proc. Int. Cong. Catal., 8th* **1984**, *5*, 183.
(71) Poliakoff, M.; Turner, J. J. *J. Chem. Soc. A* **1971**, 654.
(72) Schay, Z.; Lazar, K.; Mink, J.; Guczi, L. *J. Catal.* **1984**, *87*, 179.
(73) Theolier, A.; Choplin, A.; D'Ornelas, L.; Basset, J. M. *Polyhedron* **1983**, *2*, 119.
(74) Giannelis, E. P.; Rightor, E. G.; Pinnavaia, T. J. *J. Am. Chem. Soc.*, submitted for publication.
(75) Malik, S. K.; Poe, A. *Inorg. Chem.* **1978**, *17*, 1484.
(76) Pierantozzi, R.; Valagene, E. G.; Nordquist, A. F.; Dyer, P. N. *J. Mol. Catal.* **1983**, *21*, 189.
(77) Taure, D. J.; Rokicki, A.; Anstock, M.; Ford, P. C. *Inorg. Chem.* **1987**, *26*, 526.
(78) Johnson, B. F. G.; Lewis, J.; Raithby, P. R.; Suss, G. *J. Chem. Soc., Dalton Trans.* **1979**, 1356.
(79) Johnson, B. F. G.; Johnson, R. D.; Lewis, J.; Robinson, B. H.; Wilkinson, G. *J. Chem. Soc. A* **1968**, 2856.
(80) Johnson, B. F. G.; Lewis, J.; Williams, I. G. *J. Chem. Soc. A* **1970**, 901.
(81) Knox, S. A. R.; Koepke, J. W.; Andrews, M. A.; Kaesz, H. D. *J. Am. Chem. Soc.* **1975**, *97*, 3942.
(82) Besson, B.; Moraweck, B.; Smith, A. K.; Basset, J. M. *J. Chem. Soc., Chem. Commun.* **1980**, 569.
(83) Koepke, J. W.; Johnson, J. R.; Knox, S. A. R.; Kaesz, H. D. *J. Am. Chem. Soc.* **1975**, *97*, 3947.
(84) Budge, J. R.; Scott, J. P.; Gates, B. C. *J. Chem. Soc., Chem. Commun.* **1983**, 342.

Table IV. Summary of Reported IR Bands (cm^{-1}) of Ruthenium Carbonyls in Solution

cluster in soln	IR bands	ref
$Ru^0(CO)_5$	2035, *1999*[a]	64–67
$Ru^0(CO)_4(PF_3)$	2106, 2087, *2041*, 2027	67
$Ru^0(CO)_3(PF_3)_2$	2084, 2071, *2041*, 2026	67
$Ru^0(CO)_2(PF_3)_3$	2078, *2038*, 2026, 2007	67
$[Ru^0(CO)_2(SPh)_2]_n$	2105, *2042*, *1985*, 1945	39
$[Ru^0(CO)_2(SBu)_2]_n$	2100, *2022*, *1962*	39
$[Ru^0(CO)_2(SEL)_2]_n$	2096, *2023*, *1963*	39
$Ru^{II}(CO)_4(Cl,Br,I)_2$	2180–2160, *2105–2138*, 2095–2113, 2060–2080	39, 67–69
$Ru^{II}(CO)_3(PPh_3)(Cl,Br,I)_2$	2116–2113, 2060–2075, 2033–2037	69
$Ru^{II}(CO)_3(I,Br,Cl)_2$	*2116–2136*, *2059–2075*, 2001–2017	23, 39, 68, 69
$Ru^{II}(CO)_2(PPh_3)(I,Br,Cl)_2$	*2059–2076*, *2006–2016*	69
$[Ru^{II}(CO)_2Cl_2]_2$	2139–2140, 2078–2092, 2066–2067	67
$Ru^{II}(CO)_2(Cl,I)_2$	*2050–2063*, *1989–1995*	23, 69
$Ru_3(CO)_{12}$	*2055–2063*, *2026–2033*, 2007–2017	39, 64–68, 70–74
$Ru_3(CO)_{11}(PPh_3)$	2097–2099, *2046–2055*, *2014–2022*, 1996	75
$Ru_3(CO)_{10}(PPh_3)_2$	2080–2089, *2029–2038*, *2005–2010*, 1984	75
$Ru_3(CO)_9(PPh_3)_3$	*1985–2001*, *1975–1985*, 1970	39, 75
$Ru_3(CO)_9(PBu_3)_3$	*2035*, *1964*, 1930	39
$[HRu_3(CO)_{11}]^-$	2064–2075, *2006–2018*, *1983–1986*, 1945–1962	25, 76–78
$H_2Ru_4(CO)_{13}$	*2078–2083*, *2068*, *2056*, *2021–2026*, 2007	39, 68, 79, 80
$H_4Ru_4(CO)_{12}$	2079–2081, *2064–2068*, 2028–2034, *2022–2027*, 2007	65, 68, 79, 81, 82
$H_4Ru_4(CO)_{11}(PPh_3)$	2086, *2067*, *2057*, *2027*, *2008*	32
$H_4Ru_4(CO)_9(PPh_3)_3$	*2068*, *2024*, *2003*, *1993*, *1963*	32
$H_4Ru_4(CO)_8(PPh_3)_4$	*2015*, 1984, 1952, 1930	32
$[H_3Ru_4(CO)_{12}]^-$	2071, *2034–2040*, *2019*, *2000–2004*, 1972–1978	76, 83
$[HRu_4(CO)_{13}]^-$	*2020*, *2000*, 1970	84
$Ru_5C(CO)_{15}$	2066–2067, *2034*, 2015–2016	39, 65
$H_2Ru_5(CO)_{15}C$	*2079*, *2070*, *2062*, *2060*, 2048, 2027	65
$Ru_6(CO)_{17}C$	*2064–2066*, *2045–2049*, 2007, 1993	39, 65
$H_2Ru_6(CO)_{18}$	2067, *2058–2060*, *2052–2054*, 2003–2008	39, 65
$[Ru_6(CO)_{18}]^{2-}$	*2002*, *1990*, *1970*	76
$[Ru_6(CO)_{16}C]^{2-}$	2040, *1978*, 1921, *1820*	76

[a] Italic numbers denote strong bands.

Table V. Activation Energies and Rate Constants for Decarbonylation of Carbon-Supported Ruthenium Carbonyls in H_2 and He

species	wave-number, cm^{-1}	rate consts (at 350 K) of decarbonylation, min^{-1}		activatn energy of decarbonylation, kcal/mol	
		He	H_2	He	H_2
$H_4Ru_4(CO)_{12}$	2077		0.0080		21
$H_4Ru_4(CO)_{12}$	2064		0.0053		22
$Ru_3(CO)_{12}$	2060	0.074		21	
$Ru_3(CO)_{12}$	2027	0.041		20	
$H_4Ru_4(CO)_{12}$	2022		0.0045		18

between 330 and 373 K, a broad band in the 2010–2040-cm^{-1} region was invariably found, but the intensity of this band was low and never reached more than 10% of the original intensity. Assuming a first-order rate process, as expected for ligand dissociation or metal-metal-bond cleavage reactions,[85] the rate constants for decarbonylation were determined from the initial slopes of the relative decay of peak intensities at 2060 and 2027 cm^{-1} versus time, as illustrated in Figure 2. The intensity decay of each of these frequencies was described well by first-order kinetics in the initial stages of decarbonylation, but changes in the slope became apparent with increasing time due to the accumulation of the product giving this new overlapping band.

The decarbonylation of $Ru_3(CO)_{12}$ in H_2 at 338 K is shown in Figure 3. The spectrum of the cluster in H_2 at 300 K (not shown) exhibited bands at 2060, 2027, and 2010 cm^{-1}, indicative of $Ru_3(CO)_{12}$, but after the sample was heated in H_2 to 338 K, the $Ru_3(CO)_{12}$ was no longer present, and it had converted in 10 min to a species with infrared (IR) bands at 2077, 2064, and 2021 cm^{-1}, henceforth referred to as species S1. The transformation

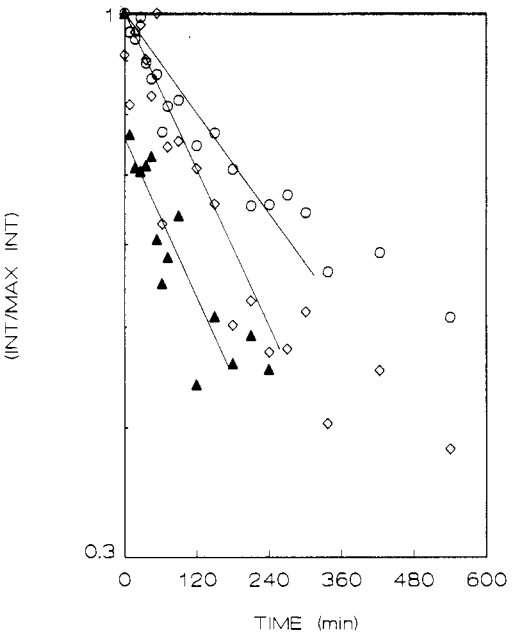

Figure 4. Rate of decarbonylation of carbon-supported $Ru_3(CO)_{12}$ in H_2 at 313 K: ◇, band at 2077 cm^{-1}; ○, band at 2064 cm^{-1}; ▲, band at 2022 cm^{-1}.

of $Ru_3(CO)_{12}$ into S1 was not limited to this run alone, but it occurred in all the decarbonylation runs in H_2 between 328 and 373 K. The decarbonylation of this species in H_2 was then followed, as shown in Figure 3, and was found to proceed significantly slower than that of $Ru_3(CO)_{12}$ in He. The formation of a final stable product with an IR band around 2040 cm^{-1} was observed. Assuming once again that decarbonylation is a first-order process, the rate constants for this process were determined from plots such as those in Figure 4, which show that decarbonylation of S1 up

(85) Geoffroy, G. L.; Wrighton, M. S. *Organometallic Photochemistry*; Academic Press: New York, 1979.

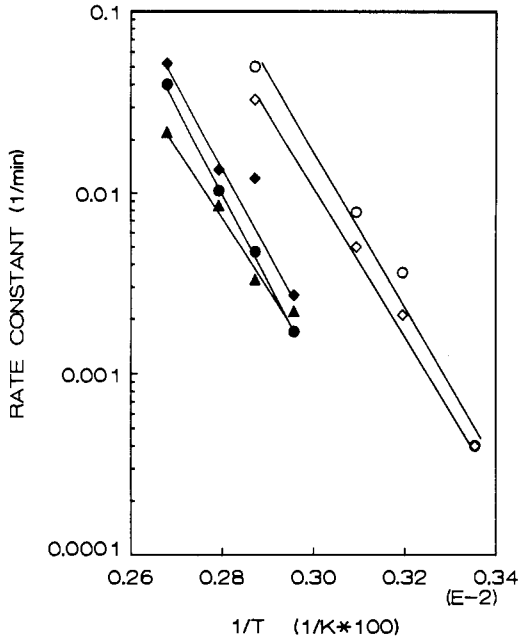

Figure 5. Arrhenius plot for the decarbonylation of carbon-supported $Ru_3(CO)_{12}$ and $H_4Ru_4(CO)_{12}$: ○, 2060-cm^{-1} band in He; ◇, 2027-cm^{-1} band in He; ◆, 2077-cm^{-1} band in H_2; ●, 2064-cm^{-1} band in H_2; ▲, 2010-cm^{-1} band in H_2.

Table VI. Summary of the Reported Heats of Adsorption of CO on Ru

ref	metal	technique[a]	Q_{ad}, kcal/mol	comments
127	Ru(1010)	FD	30	low θ
128	Ru(001)	isostere	24, 28	low θ
129	Ru(101)	FD	25, 28	
130	Ru(001)	FD	29	low θ
131	Ru(001)	TPD	25, 29	
94	1% Ru/Al_2O_3	IR, ads	25	L–H rate eq[b]
132	Ru(100)	TPD	25, 30	
133	Ru(001)	TPD	25, 29	
134	Ru(101)	TPD	25, 28	
135	Ru(110)	TPD	24–39	
136	Ru(100)		29.6	$\theta \leq 0.6$
136	Ru(100)		22.2	$\theta \leq 0.6$
136	Ru(100)	TPD	24, 28	

[a] FD = flash desorption; TPD = temperature-programmed desorption. [b] L–H = Langmuir–Hinshelwood.

to 300 min was adequately described by first-order kinetics. These rate constants gave well-behaved Arrhenius plots, shown in Figure 5, which were used to determine the activation energies for decarbonylation of $Ru_3(CO)_{12}$ in He and for S1 in H_2. The S1 species decomposed much slower than $Ru_3(CO)_{12}$ in He, but the activation energies for S1 (18–22 kcal/mol) were very similar to those obtained for $Ru_3(CO)_{12}$ in He (20–21 kcal/mol), as seen in Table V. The assignment of species S1 will be discussed later.

Following the decarbonylation runs, the catalysts were heated to 673 K in either H_2 or He, kept at 673 K for 16 h, and cooled to 300 K in this gas, after which the spectra for adsorbed CO at 300 K were obtained by exposing the sample to 11 Torr CO for 2 h in a flowing mixture, purging for 30 min, and then scanning. In order to establish the position of the band associated with linearly adsorbed CO on metallic Ru, a preliminary run was done on $Ru_3(CO)_{12}$ diluted with CaF_2 (no carbon present) by reducing the Ru MCC and exposing the reduced metal to CO in H_2 at 300 K. The spectrum, shown in Figure 6a, indicated that only a single major peak at 2024 cm^{-1} was present along with a broad peak extending below 2000 cm^{-1}. The former is associated with linear CO, while the latter is attributed to bridged CO on metallic Ru.[86] The spectrum of CO adsorbed on carbon-supported Ru after HTR,

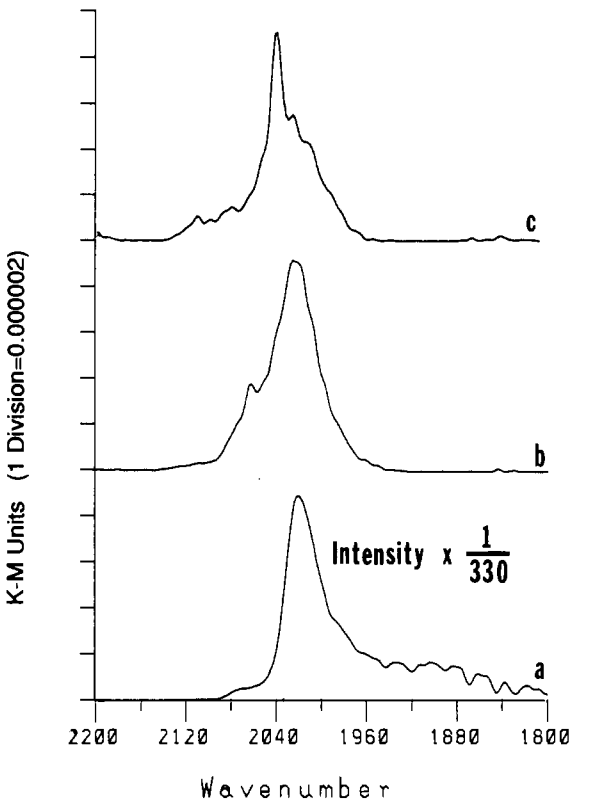

Figure 6. Spectra of CO adsorbed on Ru crystallites at 300 K: (a) CaF_2-diluted $Ru_3(CO)_{12}$ following HTR (intensity attenuated 33-fold); (b) Ru/C following 16-h reduction in H_2 at 463 K; (c) Ru/C following 16-h treatment in He at 673 K, after exposure to CO at 11 Torr in flowing H_2 and purging.

shown in Figure 6b, indicates the presence of two bands at 2062 and 2024 cm^{-1}. The band at 2024 cm^{-1} is in good agreement with reported values of 2020–2022 cm^{-1} for terminally adsorbed CO on Ru(001) crystals and Ru films,[87,88] 2010–2043 cm^{-1} for linearly adsorbed CO on reduced, Al_2O_3-supported Ru,[12,64,76,89–94] and 2000–2040 cm^{-1} for SiO_2-supported Ru.[67,73,95–104] The weak peak at 2062 cm^{-1} can be assigned to linearly adsorbed CO on positive-valent Ru atoms,[96,103] but it could also represent the formation of ruthenium subcarbonyl species. Regardless, its low intensity shows the carbon-supported Ru was well reduced. The spectrum of CO adsorbed on a Ru/C catalyst after decarbonylation in He, treatment in He at 673 K, and subsequent CO adsorption at 300 K in He is shown in Figure 6c. Two bands at 2041 and 2024 cm^{-1} can be observed, with the band at 2024 cm^{-1} again attributed to linearly adsorbed CO on metallic Ru, while the 2041 band is associated with CO on the carbon support because this band was detected on a C + CaF_2 sample containing no Ru. This 2041-cm^{-1} band was sometimes observed when short purge times were used.

(86) Sheppard, N.; Nguyen, T. T. *Adv. Infrared Raman Spectrosc.* **1978**, *5*, 67.
(87) Hollins, P.; Pritchard, J. *Prog. Surf. Sci.* **1985**, *19*, 275.
(88) Blyholder, G.; Allen, C. *J. Am. Chem. Soc.* **1969**, *91*, 3158.
(89) Kellner, C. S.; Bell, A. T. *J. Catal.* **1982**, *75*, 251.
(90) Mori, T.; Miyamoto, A.; Nizuma, H.; Takahashi, N.; Hattori, T.; Murakami, Y. *J. Phys. Chem.* **1986**, *90*, 109.
(91) Mori, T.; Miyamoto, A.; Takahashi, N.; Fukagaya, M.; Niizuma, H.; Hattori, T. *J. Chem. Soc., Chem. Commun.* **1984**, 678.
(92) Okuhara, T.; Tamura, H.; Misono, M. *J. Catal.* **1985**, *95*, 41.
(93) Dalla Betta, R. A.; Shelef, M. *J. Catal.* **1977**, *48*, 111.
(94) Kellner, C. S.; Bell, A. T. *J. Catal.* **1981**, *71*, 296.
(95) Boszormenyi, I.; Dobos, S.; Lazar, K.; Schay, Z.; Guczi, L. *Surf. Sci.* **1985**, *156*, 995.
(96) Kobayashi, M.; Shirasaki, T. *J. Catal.* **1973**, *28*, 289.
(97) Unland, M. L. *J. Catal.* **1973**, *31*, 459.
(98) Brown, M. F.; Gonzalez, R. D. *J. Catal.* **1976**, *44*, 477.
(99) Kobayashi, M.; Shirasaki, T. *J. Catal.* **1974**, *32*, 254.
(100) Kavtaradze, N. N.; Sokolova, N. P. *Dokl. Phys. Chem.* (*Engl. Transl.*) **1965**, *162*, 423.
(101) Brown, M. F.; Gonzalez, R. D. *J. Phys. Chem.* **1976**, *80*, 1731.
(102) Ekerdt, J. G.; Bell, A. T. *J. Catal.* **1979**, *58*, 170.
(103) Goodwin, J. G.; Naccache, C. *Appl. Catal.* **1982**, *4*, 145.
(104) Davydov, A. A.; Bell, A. T. *J. Catal.* **1977**, *49*, 332.

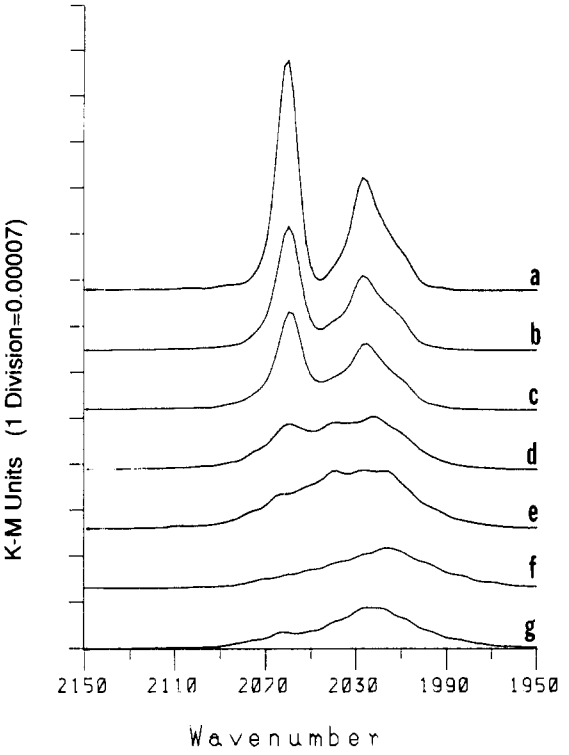

Figure 7. Spectra of carbon-supported $Ru_3(CO)_{12}$ in He at increasing temperatures: (a) 298 K, 30 min; (b) 323 K, 60 min; (c) 348 K, 10 min; (d) 348 K, 42 min; (e) 373 K, 10 min; (f) 373 K, 60 min; (g) CO adsorption at 300 K following HTR.

The $Ru_3(CO)_{12}$ therefore eventually decomposed to metallic Ru, under either flowing He or H_2.

In order to better understand the nature of the products formed during decarbonylation in He, a single sample was decomposed at increasingly higher temperatures, as shown in Figure 7. The initial cluster in He at 300 K (Figure 7a) confirmed the presence of $Ru_3(CO)_{12}$. Heating to 323 K for 60 min reduced the intensities, but the general features of the original cluster spectrum remained, as also observed in the initial spectrum at 348 K. Decarbonylation at this temperature for 42 min led to a very broad spectrum between 2070 and 1990 cm^{-1}. Heating the sample to 373 K and decarbonylating for an additional 60 min showed that the intensity of the region between 2030 and 2050 cm^{-1} decreased while the peak at 2015 cm^{-1} remained. For comparison, Figure 7g shows the spectrum obtained for CO adsorbed on the catalyst reduced in H_2. The resemblance between spectra f and g leads to the conclusion that the end product of decarbonylation in He is metallic Ru particles covered with linearly adsorbed CO. The intensity of spectrum f is roughly 10% that of spectrum a. The Ru:CO ratio is 1:4 in $Ru_3(CO)_{12}$, and it is 1:1 for linearly adsorbed CO; consequently, assuming comparable extinction coefficients, the final intensity ratio of 0.1 would indicate that 40% of the Ru atoms were surface atoms associated with linearly adsorbed CO. This value is very consistent with the Ru dispersions measured by CO adsorption (Table I), which indicate Ru crystallite sizes of 1.5–2.2 nm[3].

The catalyst was also investigated under reaction conditions, and the spectra are shown in Figure 8. Spectrum a was obtained at 473 K in flowing H_2 (749 Torr) and CO (11 Torr) after 30 min on-stream. After subtraction of gas-phase CO bands, no bands other than those for gas-phase CO_2 were detected. Heating the sample to 523 K for 30 min, however, produced CH_x stretching bands in the region of 2800–3100 cm^{-1}, and further reaction at 573 K increased the intensity of these bands at 2961, 2926, and 2867 cm^{-1}. These bands are in good agreement with reported values for methyl groups at 2875 and 2960 cm^{-1} (Figure 8c) and methylene groups at 2925 and 2850 cm^{-1}.[105,106] No obvious bands

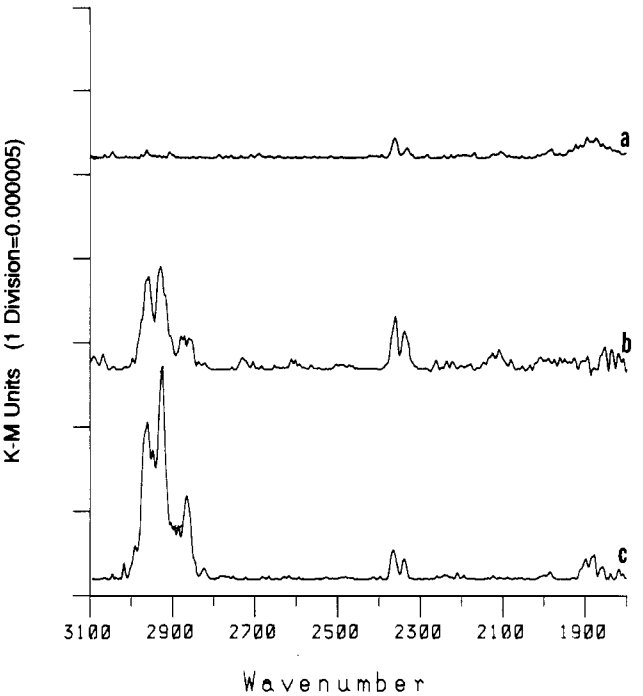

Figure 8. Spectra of carbon-supported $Ru_3(CO)_{12}$ under the following reaction conditions: (a) at 473 K after 30 min; (b) at 523 K after an additional 30 min; (c) at 573 K after an additional 30 min.

for adsorbed CO were detected under reaction conditions, presumably due to the high H_2:CO ratio of 68. The broad band at 1900 cm^{-1} is considered to be due to base-line drift and is not of sufficient resolution to be ascribed to adsorbed species.

Discussion

Although many studies of ruthenium carbonyl clusters in solution and on solid surfaces have appeared in the literature, no investigation of the thermal decomposition of any cluster has been reported. Also, no studies of the behavior of Ru clusters on carbon exist although a cluster-derived Ru/C catalyst has been prepared and characterized.[3] The highly opaque nature of carbon has successfully precluded the use of IR spectroscopy for characterization in the routine manner employed in studies of oxide-supported clusters. However, the advent of DRIFTS along with improved cells to enhance sensitivity and in situ pretreatment capabilities[49] has finally allowed the examination of C-supported clusters by an IR technique. In addition, our capability to prepare extremely clean carbon surfaces, free from oxygen-containing groups, provided the opportunity to quantitatively follow the decomposition process of these clusters in the absence of any interaction with surface oxygen. Finally, the state of the Ru particles that remain after complete decomposition was probed by looking at the IR spectra of CO chemisorbed on their surfaces, obtaining chemisorption capacities, measuring the CO heat of adsorption on these crystallites, and determining their catalytic behavior in the CO hydrogenation reaction.

Carbon supports have been shown to stabilize metals in highly dispersed forms when prepared from MCC's,[1,3-7] and the reasonably high dispersion of this Ru/C catalyst, even at a high metal loading of 8.3 wt % Ru, is further evidence of this capability. If an adsorption stoichiometry of CO:Ru_s = 1:1 (Ru_s is a surface atom) is assumed at 300 K,[3,58,93,107] dispersions were obtained of 0.57 after LTR and 0.37 after HTR, representative of 1.5–2.2-nm crystallites. After this latter pretreatment the CO adsorption values at 300 K were close to those at 195 K, implying that similar surface states existed at both these temperatures, as has been shown by IR spectra of CO on Ru films between 123 and 390 K.[100] The H_2 desorption procedure developed by Amelse et al.[53]

(105) King, D. L. *J. Catal.* **1980**, *61*, 77.

(106) Tipson, R. S. Infrared Spectroscopy of Carbohydrates. *NBS Monogr.* **1968**, *No. 110*.

(107) Guczi, L. *Catal. Rev.—Sci. Eng.* **1981**, *23*, 329.

yielded hydrogen coverages that were about half the CO coverages. Little sintering occurred during CO hydrogenation as the dispersions decreased only slightly.

Stable, active Ru catalysts have been prepared from MCC's using SiO_2, Al_2O_3, TiO_2, and zeolites,[108,109] and on oxide supports this high stability is generally ascribed to a strong interaction between the metal and surface functional groups.[110] On carbons pretreated as in this study, however, these groups are absent and the stability is attributed primarily to the high surface area of the carbon support, which gives a large pore volume within very small pores, thereby imposing physical constraints that limit migration and agglomeration. Also, the presence of active sites on the carbon surface may have helped obtain the initial high dispersions.[7]

Many studies of CO hydrogenation over Ru catalysts have now been reported from which TOF's can be obtained and compared,[3,19,46,54,89,108-125] and these numerous values have been tabulated elsewhere.[126] When extrapolated for comparison at a standard set of reaction conditions of 0.1 MPa, 548 K, and H_2:CO = 3:1, TOF values for CO conversion to hydrocarbons have typically varied from about 0.001 to near 0.7 s^{-1}. This wide range reflects the dependence of the TOF on this metal upon the Ru precursor used,[54,110-117] the support employed,[3,46,108-111,118-120] and the Ru crystallite size.[19,89,115,121-124,125] Unfortunately, more than one of these variables has frequently changed simultaneously thereby making quantitative analyses difficult; however, a couple of general statements can be made.[126] First, consistent agreement exists that a significant crystallite size effect occurs with Ru, and TOF's are 2–3 orders of magnitude lower on very small crystallites. Second, Ru dispersed on carbon has a lower TOF than Ru of similar dispersion on other supports. Consequently, the relatively low TOF's of 0.0064 s^{-1} after LTR and 0.0059 s^{-1} after HTR, the activation energies of 22–24 kcal/mol, and the absence of chain growth represent behavior in excellent agreement with previous studies of C-supported Ru.[3,19,46]

The integral CO heats of adsorption (Q_{ad}) determined calorimetrically at 300 K are listed in Table III, and reported heats of adsorption for CO on Ru single crystals are reported in Table IX. Q_{ad} for CO has been determined for Ru(1010), -(001), -(101), -(100), and -(110) single crystals, and values initially lie near 29 kcal/mol at low coverages but drop to 22–25 kcal/mol as coverages increase.[94,127-136] The integral heat of adsorption of CO on carbon-supported Ru was found to be 24.2 ± 1.6 kcal/mol CO, in excellent agreement with the values reported at high surface coverages. This consistency also indicates that the Ru was well-reduced after HTR. This heat of adsorption is lower than that of 31.3 kcal/mol obtained for an Os/C catalyst[31] and higher than the value of 15.0 kcal/mol for an Fe/C catalyst under comparable conditions.[137] Average bond strengths of 45, 41, and 30 kcal/mol have been reported for $Os_3(CO)_{12}$, $Ru_3(CO)_{12}$, and $Fe_3(CO)_{12}$, respectively;[138] therefore, this trend is very consistent with that observed for M–CO bond strengths in $M_3(CO)_{12}$ clusters.[139]

The interaction of $Ru_3(CO)_{12}$ with polymers, functionalized oxides, and oxide supports has received considerable attention.[110,140,141] In brief, the work can be summarized as follows. The interaction of $Ru_3(CO)_{12}$ with hydroxylated supports has led to a variety of surface species. Physisorbed $Ru_3(CO)_{12}$ was observed on SiO_2,[39,72] but it invariably transformed to more complex species. On Al_2O_3 physisorbed $Ru_3(CO)_{12}$ usually transformed rapidly[142] to ruthenium subcarbonyls,[40,70,95,143-145] with this decarbonylation proceeding either in a direct way from $Ru_3(CO)_{12}$ or through a relatively stable $[HRu_3(CO)_{10}(O_s)]$ intermediate[40] (O_s represents an oxygen on the support surface). This latter species was covalently bound to the surface and is analogous to the $[HOs_3(CO)_{10}(O_s)]$ species obtained after impregnation of $Os_3(CO)_{12}$.[138] On hydroxylated MgO this species was also observed,[25] but the anionic $[HRu_3(CO)_{11}]^-$ species was favored.[25,145] On hydroxylated supports the final products of cluster decomposition appear to be ruthenium subcarbonyls, assigned as Ru_A ($Ru^{III}(CO)_2$ with bands at 2138 and 2075 cm^{-1}), Ru_B ($Ru^{II}(CO)_2$ with bands at 2075 and 2008 cm^{-1}) and Ru_C ($Ru^0(CO)_2$ with bands at 2055 and 1980 cm^{-1}).[37,142] Complete decarbonylation predominantly led to Ru in a positive-valent state,[110] although reports have appeared claiming the formation of metallic Ru on Al_2O_3[40,42] and SiO_2.[72,73]

On dehydroxylated SiO_2 the physisorption of $Ru_3(CO)_{12}$ was again observed.[73,103,146] This species transformed either in a direct way[68,103] or through a $[HRu_3(CO)_{10}(O_s)]$[146] intermediate to metallic Ru. Similar reports exist for the behavior of dehydroxylated Al_2O_3,[68,76,103] although anionic $[HRu_3(CO)_{11}]^-$ was also observed.[39] The ability of dehydroxylated Al_2O_3 to stabilize anionic species is demonstrated by the presence of $[H_3Ru_4(CO)_{12}]^-$ and $[Ru_6C(CO)_{16}]^{2-}$ species.[76] Dehydroxylated MgO again formed the anionic $[HRu_3(CO)_{11}]^-$ species[25,76,145] and also stabilized the above-mentioned tetranuclear and hexanuclear anions.[76] The complete decomposition of Ru clusters on dehydroxylated supports frequently led to the formation of metallic Ru, as found on SiO_2,[68,103,146] zeolites,[147] and even Al_2O_3,[68,103] although very

(108) Chen, Y. W. *React. Kinet. Catal. Lett.* **1987**, *34*, 219.
(109) Doi, Y.; Miyake, H.; Yokota, A.; Soga, K. *J. Catal.* **1985**, *95*, 293.
(110) Brenner, A. *Metal Clusters*; John Wiley and Sons: New York, 1986; pp 249.
(111) Jackson, S. D.; Moyes, R. B.; Wells, P. B.; Whyman, R. *J. Chem. Soc., Faraday Trans.* **1987**, *83*, 905.
(112) Jordan, D. S.; Bell, A. T. *J. Phys. Chem.* **1986**, *90*, 4797.
(113) Lai, S. Y.; Vickerman, J. C. *J. Catal.* **1984**, *90*, 337.
(114) McClory, M. M.; Gonzalez, R. D. *J. Catal.* **1984**, *89*, 392.
(115) McVicker, G. B.; Vannice, M. A. *J. Catal.* **1980**, *63*, 25.
(116) Schay, Z.; Guczi, L. *React. Kinet. Catal. Lett.* **1980**, *14*, 207.
(117) Dantzenberg, F. M.; Helle, J. N.; van Santen, R. A.; Verbeeck, H. *J. Catal.* **1977**, *50*, 8.
(118) Berry, F. J.; Lin, L.; Liang, D.; Wang, C.; Tang, R.; Zhang, S. *Appl. Catal.* **1986**, *27*, 195.
(119) Budge, J. R.; Lucke, B. F.; Scott, J. P.; Gates, B. C. *Proc. Int. Cong. Catal., 8th* **1984**, *5*, 89.
(120) Stoop, F.; Verbiest, A. M. G.; van der Wiele, K. *Appl. Catal.* **1986**, *25*, 51.
(121) Dalla Betta, R. A.; Piken, A. G.; Shelef, M. *J. Catal.* **1974**, *35*, 54.
(122) Lin, Z. Z.; Okuhara, T.; Misono, M.; Tohji, K.; Udagawa, Y. *J. Chem. Soc., Chem. Commun.* **1986**, 1673.
(123) King, D. L. *J. Catal.* **1978**, *51*, 386.
(124) Peden, C. H. F.; Goodman, D. W. *ACS Symp. Ser.* **1985** *No. 288*, 185.
(125) Vannice, M. A. *J. Catal.* **1977**, *50*, 228.
(126) Venter, J. J. Ph.D. Thesis, The Pennsylvania State University, August 1988.
(127) Ku, R.; Gjostein, N. A.; Bonzel, H. P. *Surf. Sci.* **1977**, *64*, 465.
(128) Madey, T. E.; Menzel, D. *Jpn. J. Appl. Phys. Suppl. v2 pt2* **1974**, 229.
(129) Reed, P. D.; Comrie, C. M.; Lambert, R. M. *Surf. Sci.* **1976**, *59*, 33.
(130) Schwarz, J. A.; Kelemen, S. R. *Surf. Sci.* **1979**, *87*, 510.
(131) Fuggle, J. C.; Umbach, E.; Feulner, P.; Menzel, D. *Surf. Sci.* **1977**, *64*, 69.
(132) Mills, G. A.; Steffgen, F. W. *Catal. Rev.—Sci. Eng.* **1973**, *8*, 159.
(133) Ponec, V. *Catal. Rev.—Sci. Eng.* **1978**, *18*, 151.
(134) Fischer, F.; Tropsch, H. *Brenst.-Chem.* **1926**, *7*, 97.
(135) Craxford, S. R.; Rideal, E. K. *J. Chem. Soc.* **1939**, 1604.
(136) Madey, T. E.; Menzel, D. *Proc. Int. Conf. Sol. Surf., 2nd* **1974**, 229.
(137) Venter, J. J.; Vannice, M. A. *J. Phys. Chem.*, in press.
(138) Connor, J. A. *Top. Chem.* **1972**, 71.
(139) Venter, J. J.; Vannice, M. A. *J. Catal.*, in press.
(140) Zwart, J.; Snell, R. *J. Mol. Catal.* **1985**, *30*, 305.
(141) Gates, B. C. *Metal Clusters*; John Wiley and Sons; New York, 1986; pp 283.
(142) Dobos, S.; Boszormenyi, I.; Mink, J.; Guczi, L. *Inorg. Chim. Acta* **1986**, *120*, 145.
(143) Dobos, S.; Boszormenyi, I.; Mink, J.; Guczi, L. *Inorg. Chim. Acta* **1986**, *112*, 5.
(144) Knozinger, H.; Zhao, Y.; Tesche, B.; Barth, R.; Epstein, R.; Gates, B. C. *Faraday Discuss Chem. Soc.* **1982**, *72*, 53.
(145) Choplin, A.; Huang, L.; Theolier, A.; Gallezot, P.; Basset, J. M. *J. Am. Chem. Soc.* **1986**, *108*, 4224.
(146) Robertson, J.; Webb, G. *Proc. R. Soc. London, A* **1974**, *341*, 383.

Table VII. Reported Activation Energies and First-Order Rate Constants for Nucleophilic Substitution into $Ru_3(CO)_{12}$: $Ru_3(CO)_{12} + L \rightarrow Ru_3(CO)_{11}L + CO$

L	solvent	$\Delta H^{\ddagger}$, kcal/mol	T, K	k_1,[a] $10^5 s^{-1}$	k_1(350 K),[a] min^{-1}	ref
PPh_3	$C_6H_{11}CH_3$	32.2	303	0.86	0.70	149
PPh_3	$C_6H_{11}CH_3$	32.2	318	3.8	0.24	150
PPh_2Et	$C_6H_{11}CH_3$	29.7	318	3.6	0.16	150
$PPhEt_2$	$C_6H_{11}CH_3$		318	2.3	0.15	150
PEt_3	$C_6H_{11}CH_3$		318	4.1	0.26	150
PBu_3	$C_6H_{11}CH_3$		318	6.2	0.39	150
$AsPh_3$	C_6H_6		318	3.9	0.25	150
$SbPh_3$	C_6H_6		318	3.7	0.24	150
$P(OPh)_3$	$C_6H_{11}CH_3$		318	1.5	0.10	150
PPh_3	Decalin	32.2	350	250	0.15	75
$AsPh_3$	Decalin	32.7	350	260	0.16	75
$P(OPh)_3$	Decalin	32.5	350	210	0.13	75
$P\{(OCH_2)_3Et\}$	Decalin	30.3	350	330	0.20	75
CO	Decalin	31.8	323	5.6	0.15	153

[a] First-order rate constants.

stable ruthenium subcarbonyls have also been reported.[39] In summary, $Ru_3(CO)_{12}$, $[HRu_3(CO)_{11}]^-$, $[HRu_3(CO)_{10}(O_s)]$, Ru_A, Ru_B, and Ru_C have been the species detected on both hydroxylated and dehydroxylated supports. The decomposition of $Ru_3(CO)_{12}$ on oxide supports has yielded subcarbonyl species, but with the Ru mainly in oxidized form. No reports exist on the formation of $Ru^0(CO)_{5-n}L_n$ species other than the few reports of Ru_C. The decomposition of $Ru_3(CO)_{12}$ directly to metallic Ru has been reported, but its occurrence is relatively rare. The IR bands of these species are summarized in Table IV.

The decarbonylation of carbon-supported $Ru_3(CO)_{12}$ in He is shown in Figure 1. During the initial stages of decarbonylation only $Ru_3(CO)_{12}$ is present, and the decarbonylation process can be described quite well by using first-order kinetics. As shown in Figure 1, however, a small amount of product remains that eventually transforms into metallic Ru covered with CO, as indicated in Figure 7. The mechanism of decarbonylation, and thermal decomposition in general, is thus of interest as no kinetic studies of this process have appeared in the literature. It has been shown for $Ru_3(CO)_{12}$ in solution that the initial step in either substitution or fragmentation reactions of this MCC is invariably the rupture of a Ru–CO ligand, which can occur via an associative mechanism, where the incorporation of L precedes the final rupture of the Ru–CO bond, or a dissociative mechanism, where the rupture of the Ru–CO bond precedes the formation of the Ru–L bond. This behavior leads to observed rate constants of the form $k_{obs} = k_0 = k_1 + k_2[L]$,[75,148-156] where L is the entering ligand, k_1 is the first-order rate constant for the dissociative mechanism, and k_2 is the second-order rate constant for the associative mechanism. The value of k_2 depends greatly on the character of L, as k_2 is of importance for more basic ligands but is negligible for less nucleophilic ligands, although weak nucleophiles such as PPh_3 have produced a detectable $k_2[L]$ term when they were present in significant concentrations.[148]

The mechanism that has been proposed for nucleophilic attack from previous studies indicates that successive substitutions of L into MCC's can take place concurrently with cluster fragmentation to $Ru(CO)_4L$ and $Ru(CO)_3L_2$ species, and the relative importance of these two reactions depends on the nature of L.[148] When L is a weak nucleophile like PPh_3 ($P(C_6H_5)_3$), the predominant mechanism is the formation of $Ru_3(CO)_9L_3$, which then fragments slowly to $Ru(CO)_3L_2$,[149,150] but when PBu_3 ($P(C_4H_9)_3$) is used, the predominant pathway is the formation of $Ru_3(CO)_{11}L$, which then fragments rapidly to $Ru(CO)_4L$.[156] In either case the initial step is the removal of a CO molecule from $Ru_3(CO)_{12}$, and some representative values of the rate constants of this process in solution are summarized in Table VII. They show that the rate constants at 350 K are typically near 0.2 ± 0.1 min^{-1} and rather insensitive to either the solvent or L. This range of rate constants almost overlaps the value of 0.074 min^{-1} associated with the disappearance of the more intense 2060-cm^{-1} band during the decarbonylation of carbon-supported $Ru_3(CO)_{12}$ in He. This strong similarity suggests that the thermal decomposition of $Ru_3(CO)_{12}$ on carbon is initiated by loss of a CO molecule and that the carbon surface has little, if any, influence on the kinetics. The activation energies for these substitution reactions in solution, however, range from 30 to 33 kcal/mol and are substantially higher than the values of 20–21 kcal/mol obtained for thermal decomposition of C-supported $Ru_3(CO)_{12}$ in He.

Table VIII. Reported Activation Energies and First-Order Rate Constants for Nucleophilic Substitution into $Ru_3(CO)_{12-n}L_n$: $Ru_3(CO)_{12-n}L_n + L \rightarrow Ru_3(CO)_{11-n}L_{n+1} + CO$

n	L	solvent	$\Delta H^{\ddagger}$, kcal/mol	T, K	k_1, $10^5 s^{-1}$	k_1(350 K), min^{-1}	ref
0	CO	Decalin	31.8	323	56	0.15	153
1	CO	Decalin	25.6	323	340	4.3	153
2	CO	Decalin	27.9	323	220	3.7	153
1	PPh_3	Decalin	31.8	323	0.2	0.005	153
2	PPh_3	Decalin	26.4	323	7.0	0.010	153
3	PPh_3	Decalin	29.4	323	40.0	0.80	153
2	dppm	C_6H_6	25.0	343	728	0.91	154
3	dppm	C_6H_6	31.0	343	196	0.29	154

Table IX. Reported Activation Energies and First-Order Rate Constants for Fragmentation of $Ru_3(CO)_{12}$: $Ru_3(CO)_{12-n}L_n \rightarrow Ru(CO)_4L$

L	solvent	$\Delta H^{\ddagger}$, kcal/mol	T, K	k_1, $10^5 s^{-1}$	k_1(350 K), min^{-1}	ref
PBu_3	Decalin		350	140	0.085	156
PPh_3	Decalin	30.1	333	76	0.41	157
$PMePh_2$	Decalin	29.7	333	29	0.15	157
PBu_3	Decalin	31.6	333	13	0.080	157

Table X. Reported Activation Energies and First-Order Rate Constants for Substitution into $Ru(CO)_5$: $Ru(CO)_4L + L \rightarrow Ru(CO)_3L_2 + CO$

n	L	solvent	$\Delta H^{\ddagger}$, kcal/mol	T, K	k_1, $10^5 s^{-1}$	k_1(350 K), min^{-1}	ref
1	PPh_3	Decalin	25.6				155
2	PPh_3	Decalin	27.9				155
3	PPh_3	Decalin	33.0				155
3	$P(OPh)_3$	Decalin	27.4	473	124	0.000 08	155
3	PBu_3	Decalin	19.5	423	2050	0.009 6	155
1	PPh_3	Decalin	20[a]	323	2000	13.3	156
1	PPh_3	Decalin	20.7	373	5.0	0.000 5	153
2	PPh_3	Decalin	29.7	373	0.5	0.000 02	153
3	PPh_3	Decalin	35.3	373	0.05	0.000 01	153

[a] Assumed in order to calculate k_1 at 350 K.

Reactions beyond the removal of the first CO ligand can proceed via two paths, namely further substitution or fragmentation, and reported rates of substitution into Ru_3 clusters and their activation energies are listed in Table VIII. With PPh_3 as L, $Ru_3(CO)_{11}L$ rapidly forms $Ru_3(CO)_9L_3$ as the rate constants increase by a factor of 160 when going from $n = 1$ to $n = 3$. The rate constants obtained for the fragmentation of $Ru_3(CO)_{12-n}L_n$ species are shown in Table IX, and it appears that with L = PPh_3 the subsequent fragmentation is extremely slow; however, the

(147) Ballivet-Tkatchenko, D.; Tkatchenko, I. *J. Mol. Catal.* **1981**, *13*, 1.
(148) Poe, A. J. *Metal Clusters*; John Wiley and Sons: New York, 1986; pp 53.
(149) Shojaie, R.; Atwood, J. D. *Inorg. Chem.* **1987**, *26*, 2199.
(150) Candlin, J. P.; Shortland, A. C. *J. Organomet. Chem.* **1969**, *16*, 289.
(151) Shojaie, A.; Atwood, J. D. *Organometallics* **1985**, *4*, 187.
(152) Keeton, D. P.; Malik, S. K.; Poe, A. *J. Chem. Soc., Dalton Trans.* **1977**, 233.
(153) Malik, S. K.; Poe, A. *Inorg. Chem.* **1978**, *17*, 1484.
(154) Ambwani, B.; Chawla, S.; Poe, A. *Inorg. Chem.* **1985**, *24*, 2635.
(155) Malik, S. K.; Poe, A. *Inorg. Chem.* **1979**, *18*, 1241.
(156) Poe, A.; Twigg, M. V. *Inorg. Chem.* **1974**, *13*, 2982.
(157) Johnson, B. F. G.; Lewis, J.; Twigg, M. V. *J. Chem. Soc., Dalton Trans.* **1975**, 1876.
(158) Takahashi, N.; Mori, T.; Miyamoto, A.; Hattori, T.; Murakami, Y. *Appl. Catal.* **1986**, *22*, 137.

fragmentation can proceed very rapidly when L = PBu_3. Clearly, the nature of L is very important in determining the preferable path. Once fragmented, the $Ru(CO)_4L$ species can undergo further substitution, for which the rate constants are shown in Table X. Further substitution into Ru_1 clusters proceeds with rates and activation energies comparable to those for substitution into $Ru_3(CO)_{12}$. Cluster decomposition in He has been modeled from a set of irreversible steps based on proposed mechanisms,[148] in which it was assumed that first the decarbonylation steps predominate and then the fragmentation steps occur. These computer simulations using the appropriate rate constants from Tables VII–X showed that only the latter model generated the monatomic species providing the residual bands in Figure 1.[126]

The decomposition in H_2 proceeded via an entirely different path, which involved the rapid formation of a species (S1) with characteristic bands at 2077, 2064 (s), and 2021 (s) cm^{-1}. A comparison of these bands with those of Ru clusters in solution (Table IV) indicates the most probable assignment is that of $H_4Ru_4(CO)_{12}$. In order to form this MCC from $Ru_3(CO)_{12}$, both H_2 incorporation and an increase in cluster nuclearity must occur, and both have been reported in solution. The transformation of $Ru_3(CO)_{12}$ into $H_4Ru_4(CO)_{12}$ is well-established,[79-81,159,160] with the most important work being that of Knox et al., who showed this reaction occurred in octane at 393 K under flowing H_2 at 1 atm.[81] This process seems to occur via cluster fragmentation followed by aggregation because $H_4Ru_4(CO)_{12}$ has also been formed from $FeRu_2(CO)_{12}$ under the same conditions.[148] H_2 incorporation in supported clusters has also been observed as $[HRuOs_3(CO)_{12}]^-$, formed from Al_2O_3-supported $H_2RuOs_3(CO)_{12}$, reversibly incorporated H_2 under H_2 and CO to form $[H_3RuOs_3(CO)_{12}]^-$.[161]

In order for this chemistry to explain our results, the transformation to $H_4Ru_4(CO)_{12}$ must readily occur, but hydrogen incorporation in Ru clusters is known to proceed rapidly; for example, $H_2Ru_3(CO)_{10}$ is unstable at 373 K and quickly reacts with H_2 to form $H_4Ru_4(CO)_{12}$.[148] Also, the rate constant for H^+ incorporation into $[H_3Ru_4(CO)_{12}]^-$ in CH_3OH was found to be 4.8 min^{-1} at 298 K,[161,162] and if an activation energy of 20 kcal/mol from Table V is used, this rate constant at 350 K is 730 min^{-1}, 5000 times larger than the rate constants observed for CO substitution. The significant differences in the observed rates of decarbonylation of C-supported $Ru_3(CO)_{12}$ in He and H_2 can therefore be ascribed to the existence of two separate species that decarbonylate at their own characteristic rates, with $H_4Ru_4(CO)_{12}$ forming rapidly under H_2 and being more stable than $Ru_3(CO)_{12}$ due to its increased nuclearity and the enhanced stability associated with tetrahedral bonding.[70]

The activation energies observed for the thermal decomposition process, 20–21 kcal/mol for $Ru_3(CO)_{12}$ in He and 18–22 kcal/mol for $H_4Ru_4(CO)_{12}$ in H_2, are somewhat lower than the values of 30–33 kcal/mol for substitution reactions in solution (Table VII). Although these are not identical processes, it is useful to compare these values. An important point to mention is that the measured activation energies are not unreasonably low; for example, the exchange of ^{12}CO with ^{13}CO in $[HRu_3(CO)_{11}]^-$ occurs with an activation energy of 19.8 ± 0.6 kcal/mol although the rate constant for exchange is much higher.[163]

The most feasible explanation for the lower activation energies is that the reaction on carbon produces metallic Ru particles; thus, the energy required to break the Ru–CO bond is partly provided by rapid Ru–Ru bond formation. If this is the case, thermodynamic pathways can be associated with these energy changes, as shown in Figure 9, where n $Ru_3(CO)_{12}$ molecules eventually form $12n$ CO gas-phase molecules and a Ru_{3n} particle. Assuming Ru–Ru and Ru–CO bond energies of 28 and 41 kcal/mol, respectively,[138] Q_2 is 48 kcal/mol by using the equation in Figure 9. The net energy change for the overall process, Q_1, is then obtained by subtracting the heat of formation of Ru_{3n} from Q_2. Two limiting cases can be proposed. The first assumes that formation of bulk hcp Ru occurs, in which case each Ru atom has 12 nearest neighbors and the condensation energy is the cohesive energy density of 155 kcal/mol.[164] This leads to Q_1 = 9.3 kcal/mol and an estimate of the minimum activation energy for this endothermic step. The second case assumes that only small metal aggregates form, in which Ru–Ru bond strengths of 28 kcal/mol are maintained, and each Ru atom has z nearest neighbors. Q_1 is then $48 - (3/12)[(0.5)(28)z] = 48 - 3.5z$. An activation energy of 20–22 kcal/mol requires z to be 7–8, which is a very reasonable coordination number for surface Ru atoms, which predominate in these small clusters. These arguments show that the measured activation energies are reasonable for this endothermic process.

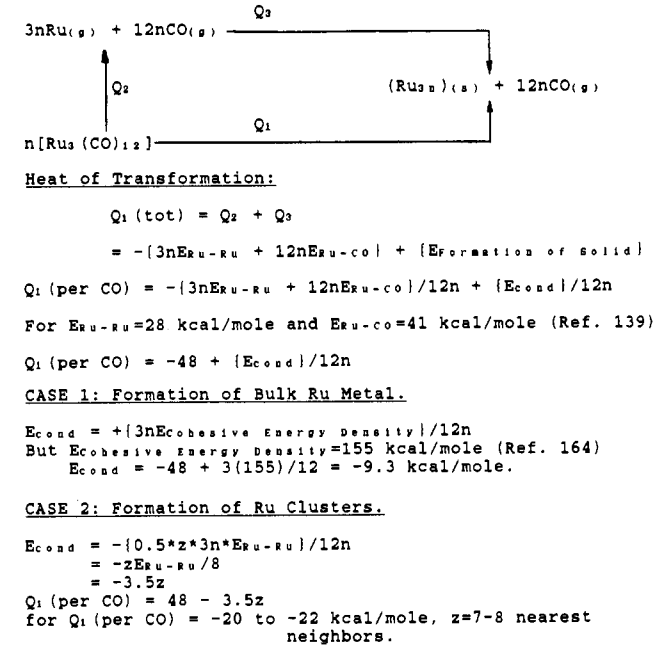

Figure 9. Thermodynamic path to estimate the minimum activation energies of decarbonylation. E_{Ru-Ru} is the Ru–Ru bond strength in $Ru_3(CO)_{12}$; E_{Ru-CO} is the Ru–CO bond strength in $Ru_3(CO)_{12}$; E_{cond} is the energy released during the addition of a Ru atom to form a particle; z is the number of nearest neighbors in the Ru particle.

Another possible explanation is that the ligand concentration [L] distorted the total rate constant, which was represented as $k_0 = k_1 + k_2[L]$. Since only k_0 was measured, from which k_1 was determined, the implicit assumption was made that either k_2 was very small or [L] was negligible, neither of which is necessarily true. Depending on the nature of L, these effects can be pronounced. If the active sites postulated to exist on carbon[7] are strongly nucleophilic in nature and, in fact, do interact with the cluster, then the second term could have an effect on the determined activation energy.

This Ru/C catalyst was also investigated under reaction conditions, but no adsorbed CO was detected, in contradistinction with other work.[89-91,94,102,165-167] This is undoubtedly due to the extraordinarily high H_2:CO ratio of 68 used in this work. The formation of hydrocarbon products was clearly observed, however,

(159) Eady, C. R.; Johnson, B. F. G.; Lewis, J. *J. Organomet. Chem.* **1973**, *57*, C84.
(160) Piacenti, F.; Bianchi, M.; Frediani, P.; Benedetti, E. *Inorg. Chem.* **1971**, *10*, 2579.
(161) Budge, J. R.; Scott, J. P.; Gates, B. C. *J. Chem. Soc., Chem. Commun.* **1983**, 342.
(162) Walker, H. W.; Pearson, R. G.; Ford, P. C. *J. Am. Chem. Soc.* **1983**, *105*, 1179.
(163) Payne, M. W.; Leussing, D. L.; Shore, S. G. *J. Am. Chem. Soc.* **1987**, *109*, 617.
(164) Kittel, C. *Solid State Physics*; John Wiley and Sons: New York, 1976.
(165) Mori, T.; Miyamoto, A.; Takahashi, N.; Fukagaya, M.; Hattori, T. *J. Phys. Chem.* **1987**, *90*, 5197.
(166) Barteau, M. A.; Feulner, P.; Stengl, R.; Broughton, J. Q.; Menzel, D. *J. Catal.* **1985**, *94*, 51.
(167) Ekerdt, J. G.; Bell, A. T. *J. Catal.* **1980**, *62*, 19.

as bands associated with CH_x groups were visible at 2961, 2948, 2925, and 2866 cm^{-1}. These bands agree with those reported for CH_3 at 2960 and 2875 cm^{-1}, for CH_2 at 2927 and 2862 cm^{-1}, and for CH at 2950 cm^{-1}.[105,106,166] Although the location of these hydrocarbon species on the catalyst surface could not be assigned with certainty, it is clear from the relative intensities, which show that CH_3 groups predominate, that the average chain length of these species was much shorter than those observed by King et al.[105] on SiO_2-supported Ru under reaction conditions. It is presumed that these IR-detectable species are most likely carbonaceous species adsorbed on the carbon, rather than the Ru, and are not reaction intermediates, consistent with the conclusions of Ekerdt and Bell.[102,167]

Summary

DRIFTS has been successfully applied to study carbon-supported Ru cluster catalysts. The decarbonylation of $Ru_3(CO)_{12}$ was followed quantitatively, and an activation energy near 20 kcal/mol was obtained in He. However, in H_2, the $H_4Ru_4(CO)_{12}$ cluster was rapidly formed, and its subsequent decomposition also followed first-order kinetics and gave activation energy values of 18-22 kcal/mol. To the best of our knowledge, this is the first time that the thermal decomposition of any ruthenium carbonyl cluster has been quantitatively studied, either in solution or on a support. The observed behavior can be explained by assuming the rate-determining step for the decomposition of the supported cluster is the same as that for nucleophilic substitution reactions of the cluster in solution, i.e., rupture of the first Ru-CO ligand, and the decarbonylation rates were very similar to rates of substitution in solution. The measured activation energies were lower than those in solution; however, the formation of highly dispersed metallic Ru particles would be expected to lower the activation energy of decarbonylation, as shown by thermodynamic calculations. Decomposition in He appeared to proceed via decarbonylation of $Ru_3(CO)_{12}$ followed by fragmentation, whereas the rapid formation of $H_4Ru_4(CO)_{12}$ and its subsequent decomposition was observed under H_2.

Complete decarbonylation in either gas produced zerovalent Ru, and adsorption of CO on these small Ru crystallites yielded spectra in good agreement with those reported in the literature for CO adsorbed on metallic Ru. Also, the calorimetric integral heat of adsorption of CO of 24.2 kcal/mol was very reasonable compared to reported values for CO adsorbed on Ru single crystals. The chemisorption measurements showed that the Ru particles were well-dispersed and resistant to sintering, even under reaction conditions. IR spectra under reaction conditions showed frequencies associated with CH, CH_2, and CH_3 species, and the preponderance of the last indicated the presence of only short-chain hydrocarbons on the catalyst surface, most likely on the carbon. The low turnover frequencies are similar to values measured over other well-dispersed and C-supported Ru catalysts.

Acknowledgment. This study was supported by the donors of the Petroleum Research Fund, administered by the American Chemical Society, and by the NSF Kinetics and Catalysis Program through Grant No. CBT-8619619.

Contribution from the Department of Chemistry and Biochemistry, University of Windsor, Windsor, Ontario, Canada N9B 3P4

Coordination Compounds of Indium. 46. Indium(I) Derivatives of 3,5-Di-*tert*-butyl-1,2-*o*-benzoquinone

Theodore A. Annan, David H. McConville, Bruce R. McGarvey, Andrzej Ozarowski, and Dennis G. Tuck*

Received September 15, 1988

Indium metal reacts with 3,5-di-*tert*-butyl-1,2-*o*-benzoquinone (TBQ) in refluxing toluene to give a solution of the corresponding semiquinone-indium(I) complex (TBSQ)In. This species can be stabilized in the solid state as a neutral complex with 1,10-phenanthroline (phen) or as a salt of the anion $[(TBSQ)In(Cl)\cdot phen]^-$. Oxidation in solution by I_2, $(C_6H_5)_2E_2$ (E = S, Se), and $o\text{-}O_2C_6Cl_4$ gives the indium(III) products $(TBSQ)InI_2$, $(TBSQ)In(EC_6H_5)_2$, and $(TBSQ)In(O_2C_6Cl_4)$, which again can be stabilized as the phen adducts. These compounds can also be prepared directly by refluxing mixtures of (e.g.) In + TBQ + I_2. All these semiquinone compounds give electron spin resonance spectra, and the hyperfine coupling constants A_{In} confirm the formulations. There are significant changes in A_{In} values as the result of the oxidation of indium(I) to indium(III).

Introduction

Recent work in this laboratory has been concerned with the oxidative-addition reaction between tin(II)[1] or indium(I)[2] halides and substituted *o*-benzoquinones to give the corresponding substituted catecholato derivatives. With the tetrahalogeno-*o*-quinones $Y_4C_6O_2$ (Y = Cl, Br), the reaction products are either $(Y_4C_6O_2)SnX_2$ or $(Y_4C_6O_2)InX$, which have been isolated as adducts with both neutral and anionic donor ligands. When the substrate is a less easily reduced *o*-quinone, such as 3,5-di-*tert*-butyl-*o*-benzoquinone, it is possible to observe the electron spin resonance (ESR) spectrum of the appropriate metal-semiquinone compounds, and with tin and indium both higher (+IV, +III) and lower (+II, +I) oxidation state species have been detected.[3] It therefore became important to investigate the preparation and properties of these lower oxidation species, and we now report the synthesis and study of (3,5-di-*tert*-butyl-*o*-semiquinonato)indium(I).

Relatively few indium(I) complexes are known,[4] but it is worth noting that the reactions of cyclopentadienylindium(I) with a number of β-diketonates has been shown to yield the indium(I) derivatives of the corresponding bidentate monoanion.[5] The present synthesis is considerably simpler, involving merely refluxing the metal and *o*-quinone together in a suitable solvent. We have recently shown[6] that both indium and tin react directly with $(C_6H_5)_2E_2$ (E = S, Se) to give $In(EC_6H_5)_3$ or $Sn(EC_6H_5)_4$, and it may well be that the metals represent a neglected starting point for the synthesis of main-group compounds.

Experimental Section

General Data. Indium metal (Alfa) was in the form of fine shavings. Solvents were dried by conventional methods and stored over appropriate drying agents; 3,5-di-*tert*-butyl-*o*-benzoquinone and other organic reagents were used without further purification. All experiments were carried out in an atmosphere of dry nitrogen. In the subsequent text, we use the abbreviation TBQ for the parent quinone, and TBSQ for the one-elec-

(1) Annan, T. A.; Chadha, R. K.; Tuck, D. G.; Watson, K. *Can. J. Chem.* **1987**, *65*, 2670.
(2) Annan, T. A.; Tuck, D. G. *Can. J. Chem.* **1988**, *66*, 2935.
(3) Annan, T. A.; Chadha, R. K.; McConville, D. H.; McGarvey, B. R.; Ozarowski, A.; Tuck, D. G. *J. Chem. Soc., Dalton Trans.*, in press, and unpublished results.
(4) Tuck, D. G. In *Comprehensive Coordination Chemistry*; Wilkinson, G., Gillard, R. D., McCleverty, J. A., Eds.; Pergamon Press, Oxford, U.K., 1987; Vol. 3, p 154 ff.
(5) Habeeb, J. J.; Tuck, D. G. *J. Chem. Soc., Dalton Trans.* **1975**, 1815.
(6) Mabrouk, H. E.; Kumar, R.; Tuck, D. G. *J. Chem. Soc., Dalton Trans.* **1988**, 1045.

0020-1669/89/1328-1644$01.50/0